

**Working Title: Monte Carlo Analysis of Dynamic Systems**

by

Chelsea A. D'Angelo

A preliminary report submitted in partial fulfillment of  
the requirements for the degree of

Doctor of Philosophy

(Nuclear Engineering and Engineering Physics)

at the

UNIVERSITY OF WISCONSIN-MADISON

2017

Date of preliminary oral examination: 09/01/2017

Thesis Committee:

Paul P. H. Wilson, Professor, Nuclear Engineering

Douglass Henderson, Professor, Nuclear Engineering

Bryan Bednarz, Professor, Medical Physics

Andrew Davis, Associate Scientist, Engineering Physics



© Copyright by Chelsea A. D'Angelo 2017  
All Rights Reserved

## CONTENTS

---

Contents	i
List of Figures	iii
<b>1 Introduction</b>	<b>1</b>
<b>2 Literature Review</b>	<b>4</b>
2.1 <i>Shutdown Dose Rate Analysis</i> . . . . .	4
2.1.1 D1S . . . . .	4
2.1.2 R2S . . . . .	5
2.2 <i>Analog Monte Carlo Calculations</i> . . . . .	5
2.3 <i>Monte Carlo Variance Reduction Methods</i> . . . . .	6
2.4 <i>Automated Variance Reduction</i> . . . . .	8
2.4.1 CADIS . . . . .	10
2.4.2 FW-CADIS . . . . .	11
2.5 <i>Automated Variance Reduction for Multiphysics</i> . . . . .	12
2.5.1 Multi-Step CADIS . . . . .	12
2.5.2 Groupwise-Transmutation CADIS . . . . .	14
2.6 <i>Moving Geometries and Sources</i> . . . . .	15
2.6.1 MCNP6 Moving Objects Capability . . . . .	15
2.6.2 MCR2S with Geometry Movement . . . . .	16
<b>3 Experiment</b>	<b>18</b>
3.1 <i>Demonstration of GT-CADIS</i> . . . . .	18
3.1.1 Problem Description . . . . .	18
3.1.2 Analog R2S . . . . .	19
3.1.3 GT-CADIS . . . . .	19
3.2 <i>Limitations of GT-CADIS for Moving Systems</i> . . . . .	21

<b>4</b>	<b>Variance Reduction for Time-integrated Multiphysics Analysis</b>	<b>23</b>
4.1	<i>Generalized MS-CADIS Method</i> . . . . .	23
4.2	<i>Time-integrated MS-CADIS</i> . . . . .	26
4.3	<i>Time-integrated GT-CADIS</i> . . . . .	26
<b>5</b>	<b>Progress</b>	<b>28</b>
5.1	<i>DAGMC Simulations with Geometry Transformations</i> . . . . .	28
5.1.1	Production of Stepwise Geometry Files . . . . .	28
5.1.2	DAGMCNP Geometry Transformations . . . . .	28
<b>6</b>	<b>Proposal</b>	<b>30</b>
6.1	<i>TR2S</i> . . . . .	30
6.2	<i>Implementation: Time-integrated SDR Analysis</i> . . . . .	31
6.2.1	Generation of the TGT-CADIS Variance Reduction Parameters . . . . .	31
6.2.2	Optimized, Time-integrated R2S Workflow . . . . .	34
6.2.3	Error Propagation . . . . .	36
6.2.4	Assumptions and Practical Considerations . . . . .	38
6.2.4.1	Data management . . . . .	39
6.3	<i>Demonstration</i> . . . . .	40
6.3.1	Toy Problem . . . . .	40
6.3.2	Full-scale FES Model . . . . .	40
6.4	<i>Summary</i> . . . . .	41
	<b>Bibliography</b>	<b>42</b>

## LIST OF FIGURES

---

3.1	Experimental Geometry . . . . .	19
3.2	Analog neutron flux and error . . . . .	19
3.3	GT-CADIS adjoint photon flux . . . . .	20
3.4	GT-CADIS adjoint neutron flux . . . . .	20
3.5	GT-CADIS biased neutron source . . . . .	21
3.6	GT-CADIS weight window mesh . . . . .	21
3.7	GT-CADIS neutron flux and relative error . . . . .	21
3.8	GT-CADIS photon source . . . . .	21
6.1	Time-integrated R2S (TR2S) workflow . . . . .	32
6.2	Workflow to generate TGT-CADIS adjoint neutron source . . .	35
6.3	Workflow to generate TGT-CADIS biased source and weight windows . . . . .	36
6.4	Fully optimized, time-integrated R2S workflow . . . . .	37
6.5	Geometry for TGT-CADIS Demonstration . . . . .	40

## **Abstract**

### **Abstract**

Eloquent summary of my work.

## 1 INTRODUCTION

---

The successful completion of this project will provide the workflow and tools necessary to efficiently calculate quantities of interest resulting from coupled, multi-physics processes in dynamic systems. The MC physics code will be modified to implement rigid-body transformations on the CAD-based geometry. MS-CADIS, a VR method for coupled, multi-physics problems, will be adapted to incorporate dynamics. An experiment will be contrived to demonstrate the limitations of existing VR methods as they apply to dynamic problems and verify the efficacy of this new method. Given these objectives, the following chapters will include background and theory relevant to VR methods in coupled, multi-physics systems. Chapter no. will provide an introduction to computational radiation transport and specifically the VR methods used in MC calculations. Chapter no. will discuss SDR analysis and the VR methods specific to these calculations. Chapter no. will introduce radiation transport in dynamic systems, discuss how they are handled now and how motion affects VR in coupled multi-physics problems like SDR calculations. Finally, chapter no. will discuss the progress that has been made towards this new methodology and outline a proposal of the work to be done.

The rapid design iteration process of complex nuclear systems has long been aided by the use of computational simulation. Traditionally, these simulations involve radiation transport in static geometries. However, in certain scenarios, it is desirable to investigate dynamic systems and the effects caused by the motion of one or more components. For example, Fusion Energy Systems (FES) are purposefully designed with modular components that can be moved in and out of a facility after shutdown for maintenance. To ensure the safety of maintenance personnel, it is important to accurately quantify the shutdown dose rate (SDR) caused by the gammas emitted by structural materials that became activated during the



device operation time. This type of analysis requires neutron transport to determine the neutron flux, activation calculation to determine the isotopic inventory, and finally a photon transport calculation to determine the SDR. While MC calculations are revered to be the most accurate method for simulating radiation transport, the computational expense of obtaining low error results in systems with heavy shielding can be prohibitive. However there are techniques, known as variance reduction (VR) methods, that can be used to increase the computational efficiency. There are several types of VR methods, but the basic theory is to artificially increase the simulation of events that will contribute to the quantity of interest such as flux or dose rate. One class of VR techniques relies upon a deterministic estimate of the adjoint solution of the transport equation to formulate biasing parameters used in the MC transport. The adjoint flux has physical significance as the importance of a region of phase space to the objective function.

The purpose of this work is to create a methodology for the efficient calculation of quantities of interest in dynamic, geometrically complex nuclear systems. For cases involving coupled multi-physics analysis, such as SDR calculations, a new hybrid deterministic/MC VR technique will be proposed. This new method will adapt the Multi-Step Consistent Adjoint Driven Importance Sampling (MS-CADIS) method to dynamic systems. The basis of MS-CADIS is that the importance function used in each step of the problem must represent the importance of the particles to the final objective function. As the spatial configuration of the materials changes, the probability that they will contribute to the objective function also changes. In the specific case of SDR calculations, the importance function for the neutron transport step must capture the probability of materials to become activated and subsequently emit photons that will make a significant contribution to the SDR. This new VR method will also take advantage of the Groupwise Transmutation (GT)-CADIS method which is an implementation of MS-CADIS that optimizes the neutron transport

step of SDR calculations. GT-CADIS generates an adjoint neutron source based on certain assumptions and approximations about the transmutation network. To adapt this method for dynamic systems, the adjoint neutron source will be calculated at each time step and then averaged in order to generate the biasing functions for the neutron transport step.

## 2 LITERATURE REVIEW

---

The goal of this thesis work is to optimize the neutron transport step of a coupled, multi-physics process occurring in a system that has moving components. One important application of this work is the quantification of the SDR during maintenance operations in FES. This chapter intends to provide background information on SDR analysis in FES and how radiation transport calculations are currently handled in systems with moving geometries and sources.

### 2.1 Shutdown Dose Rate Analysis

Shutdown dose rate (SDR) calculations are necessary to quantify the potential dose to personnel working in facilities exposed to intense radiation fields such as those present in fusion energy systems (FES). The dose rate in these facilities is caused by decay photons that are emitted by materials irradiated by neutrons. There are two primary workflows used to investigate the SDR: the Direct 1-Step (D1S) [4] and the Rigorous 2-Step (R2S) [6] method.

#### 2.1.1 D1S

The D1S method performs coupled neutron-gamma transport in the same simulation. It relies upon a modified version of MCNP5 with special cross-section data and the FISPACT nuclear inventory code for time correction factors. The decay gammas are emitted as prompt so they can be transported at the same time as neutrons. A time correction factor is later applied. Because both neutron and photon transport occur in the same simulation, therefore on the same geometry, D1S is not currently applicable to geometries that undergo movement after shutdown. This has

been identified as a necessary improvement and the development of a subroutine to produce portable decay photon sources for pure photon calculations is underway [5].

### **2.1.2 R2S**

In contrast to D1S, the R2S method relies upon separate MC neutron and photon transport steps. The transport steps are coupled by activation analysis. The goal of the neutron transport step is to determine the neutron flux as a function of space and energy. This neutron flux along with a specific irradiation and decay scenario are used as input into a nuclear inventory code to determine the photon spectrum as a function of decay time. The calculated photon spectrum for each decay time is then used as the source for the photon transport step. A photon flux tally fitted with flux-to-dose-rate conversion factors is used during this step to determine the final SDR [6].

## **2.2 Analog Monte Carlo Calculations**

The quantification of the SDR requires a detailed distribution of first the neutron and then the photon flux throughout all regions of phase space. Due to the size and complexity of FES, the most optimal way to obtain accurate particle distributions is through MC radiation transport rather than deterministic methods \*need source\*.

In general, MC calculations rely on repeated, random sampling to solve mathematical problems. In radiation transport applications, the MC method is used to solve the Boltzmann transport equation [11] through the simulation of random particle walks through phase space. In analog operation mode (i.e. no variance reduction), the source particle's position, energy, direction and subsequent collisions are sampled from probability distribution functions (PDFs). Quantities of interest such as flux can be

scored, or tallied, by averaging particle behavior in discrete regions of phase space.

One challenge incurred by MC simulations of FES is the presence of heavily shielded regions. The particles undergo a high degree of collisions (absorption and scattering) in the shielding which results in low particle fluxes in these discrete regions of phase space. Regions that have low particle fluxes have higher statistical uncertainty.

The statistical error is a function of the relative error,  $R$ , which is defined as

$$R = \frac{S_{\bar{x}}}{\bar{x}} \quad (2.1)$$

where  $\bar{x}$  is the average of the tally scores, and  $S_{\bar{x}}$  is the standard deviation of the tally scores. For a well behaved tally,  $R$  is proportional to  $1/\sqrt{N}$  where  $N$  is the number of tally scores [3].

The relative error is inversely proportional to  $N$ . Therefore, to reliably predict results in these regions, many particle histories need to be simulated which may require large amounts of computer time.

MC calculation efficiency is measured by a quantity known as the figure of merit (FOM). The FOM is a function of relative error,  $R$ , and computer processing time,  $T$ , as given by

$$\text{FOM} = \frac{1}{R^2 T} \quad (2.2)$$

A high FOM is desirable because it means that less computation time is needed to achieve a reasonably low error, less than 0.1 according to the MCNP manual [3].

## 2.3 Monte Carlo Variance Reduction Methods

Certain MC calculations require the use of VR methods in order to complete or improve the efficiency of the calculation. As previously discussed,

the highly-attenuating configuration of FES requires the use of VR to optimize the transport. Looking to Eq. 2.2, VR methods aim to increase the FOM by increasing  $N$  and decreasing  $S_{\bar{x}}$  by preferentially sampling trajectories that are likely to contribute to the tallies of interest. This effectively forces more collisions in regions of phase space that are important to the tally of interest. This is accomplished by sampling from biased PDFs that govern particle behavior.

In order to compensate for this biased sampling, the particle statistical weight is adjusted accordingly. The relationship between the particle statistical weight,  $w$ , and the PDF that governs particle behavior is as follows

$$w_{\text{biased}} \text{pdf}_{\text{biased}} = w_{\text{unbiased}} \text{pdf}_{\text{unbiased}} \quad (2.3)$$

One of the earliest and still commonly used methods of VR is particle splitting and rouletting. This is particularly useful in deep penetration simulations, like FES where neutrons penetrate deeply into shielded regions. Generally speaking, to increase the number of particle histories that can contribute to tallies of interest, it is desirable to split particles as they enter more important regions and roulette particles as they enter less important regions. This requires assigning an importance,  $I$ , to every region in the geometry and adjusting the weight,  $w$ , of the new particles. When a particle moves from a region A to a region B, the ratio of importances is calculated. If region B is more important than region A such that  $I_B/I_A \geq 1$ , the particle with original weight  $w_0$  is split into  $n = I_B/I_A$  particles, each with weight  $w_0/n$ . If instead region B is less important than region A such that  $I_B/I_A < 1$ , the particle will undergo roulette. The particle will survive with a probability  $n$  and weight  $w_0/n$  [2]. The weight window method in the Monte Carlo N-Particle (MCNP) code utilizes both splitting and rouletting. A weight window is a region of phase-space that is assigned an upper and lower bound. The windows can be assigned to cells in the geometry, on a superimposed mesh, and to energy bins. When

a particle enters a weight window, its weight is assessed; if its weight is above the upper bound or below the lower bound, it is either split or rouletted, respectively.

## 2.4 Automated Variance Reduction

Historically, VR techniques have required a priori knowledge of the problem physics in order to assign importance parameters, therefore requiring a vast amount of user expertise and time. Many techniques have been developed over the years to automate the selection and assignment of these parameters to reduce computational and human effort.

One class of VR techniques, known as hybrid deterministic/MC methods, is based upon the solution to the adjoint Boltzmann transport equation having significance as the measure of importance of a particle to some specified objective function. Because deterministic solutions to the transport equation require much less computation time, they are useful as an estimate of the adjoint particle flux throughout phase space which can then be used to determine importance of specific regions. To demonstrate the use of the adjoint solution as an importance function, first start with the linear, time-independent Boltzmann transport equation shown below

$$H\Psi = q \quad (2.4)$$

where  $\Psi$  is the angular flux,  $q$  is the source of particles, and the operator  $H$  is given by

$$H = \hat{\Omega} \cdot \nabla + \sigma_t(\vec{r}, E) - \int_0^\infty dE' \int_{4\pi} d\Omega' \sigma_s(\vec{r}, E' \rightarrow E, \hat{\Omega}' \rightarrow \hat{\Omega}) \quad (2.5)$$

where  $\sigma_t$  is the total cross-section and  $\sigma_s$  is the differential scattering

cross-section. The adjoint identity states that

$$\langle \Psi^+, H\Psi \rangle = \langle \Psi, H^+\Psi^+ \rangle \quad (2.6)$$

where  $\langle \cdot \rangle$  refers to the integration over space, energy, and angle and the adjoint operator  $H^+$  is given by

$$H^+ = -\hat{\Omega} \cdot \nabla + \sigma_t(\vec{r}, E) - \int_0^\infty dE' \int_{4\pi} d\Omega' \sigma_s(\vec{r}, E \rightarrow E', \hat{\Omega} \rightarrow \hat{\Omega}') \quad (2.7)$$

This identity can also be written as

$$\langle \Psi^+, q \rangle = \langle \Psi, q^+ \rangle \quad (2.8)$$

As mentioned, the adjoint solution to the transport equation will be used as an importance function therefore a solution to the following equation is needed

$$H^+\Psi^+ = q^+ \quad (2.9)$$

which requires the thoughtful selection of an adjoint source  $q^+$ . To demonstrate the physical significance of the adjoint, consider the detector response,  $R$

$$R = \langle \Psi, \sigma_d \rangle \quad (2.10)$$

where  $\sigma_d$  is a detector response function. If the adjoint source is chosen to be equivalent to the detector response function,

$$q^+ = \sigma_d \quad (2.11)$$

and substituted into Eq. 2.10 and Eq. 2.8

$$R = \langle \Psi, q^+ \rangle = \langle \Psi^+, q \rangle \quad (2.12)$$

the adjoint flux  $\Psi^+$  represents the importance of a region to  $R$ . This final



relation allows us to know the response  $R$  for any source  $q$  once the adjoint flux  $\Psi^+$  for a detector of interest is known.

### 2.4.1 CADIS

The Consistent Adjoint Driven Importance Sampling (CADIS) method is one of the hybrid deterministic/MC VR techniques that uses the adjoint solution to formulate source and transport biasing parameters for MC transport. More specifically, CADIS determines the parameters for source biasing and the weight window lower bounds in a consistent manner. The response, or tally, of interest in a transport calculation can be represented by the following equation

$$R = \int_V d\vec{r} \int_E dE \int_{4\pi} d\hat{\Omega} \sigma_d(\vec{r}, E, \hat{\Omega}) \Psi(\vec{r}, E, \hat{\Omega}) \quad (2.13)$$

and in terms of the adjoint flux,

$$R = \int_V d\vec{r} \int_E dE \int_{4\pi} d\hat{\Omega} q(\vec{r}, E, \hat{\Omega}) \Psi^+(\vec{r}, E, \hat{\Omega}) \quad (2.14)$$

The MC solution of the response relies upon the sampling of the particle source distribution,  $q(\vec{r}, E, \hat{\Omega})$ , represented by a PDF. In an effort to decrease the variance, it is possible to sample from a biased PDF which is given by

$$\hat{q}(\vec{r}, E, \hat{\Omega}) = \frac{\Psi^+(\vec{r}, E, \hat{\Omega}) q(\vec{r}, E, \hat{\Omega})}{R} \quad (2.15)$$

This biased PDF represents the contribution of particles from phase space to the total detector response,  $R$ . As previously mentioned, when sampling from a biased PDF, the particle weight needs to be adjusted to eliminate systematic bias.

$$w(\vec{r}, E, \hat{\Omega}) \hat{q}(\vec{r}, E, \hat{\Omega}) = w_0 q(\vec{r}, E, \hat{\Omega}) \quad (2.16)$$

Substituting in Eq. 2.15, the corrected particle weight is shown to have an inverse relation to the adjoint flux, or importance function.

$$w(\vec{r}, E, \hat{\Omega}) = \frac{R}{\Psi^+(\vec{r}, E, \hat{\Omega})} \quad (2.17)$$

In the weight window technique, particles are either split or rouletted as they move from region to region based on the ratio of their importances and their weight is updated accordingly. The weights are used for both the source and transport biasing parameters and are derived in a consistent manner. The transport is biased according to the following relationship

$$w(\vec{r}, E, \hat{\Omega}) = w(\vec{r}', E', \hat{\Omega}') \left[ \frac{\Psi^+(\vec{r}', E', \hat{\Omega}')}{\Psi^+(\vec{r}, E, \hat{\Omega})} \right] \quad (2.18)$$

The width of the weight windows is determined by a parameter defined to be the ratio between upper and lower bounds  $\alpha = w_u/w_l$ . MCNP uses a default value for  $\alpha$  and the weight window lower bounds are given by

$$w_l(\vec{r}, E, \hat{\Omega}) = \frac{R}{\Psi^+(\vec{r}, E, \hat{\Omega})^{(\frac{\alpha+1}{2})}} \quad (2.19)$$

## 2.4.2 FW-CADIS

The Forward-Weighted CADIS method is another hybrid deterministic/MC VR method that aims to increase the efficiency of global flux or dose distributions or detector responses at multiple locations [?]. The goal is to create uniform particle density in the scoring regions such that there is uniform statistical uncertainty in the MC solution in these regions. This method relies on using a forward deterministic transport solution to weight the source for adjoint deterministic transport. The adjoint solution is then used with the standard CADIS method to produce source and transport biasing parameters for the forward MC transport simulation.

The adjoint source is given as

$$q^+ = \frac{1}{\phi(\vec{r}, E)} \quad (2.20)$$

## 2.5 Automated Variance Reduction for Multiphysics

The R2S method requires two transport steps; the initial neutron transport to simulate the irradiation and the subsequent photon transport simulating the decay photons. Applying this method to a full-scale, 3D FES becomes impractical due to the need for accurate space- and energy-dependent fluxes generated by MC codes throughout the geometry.

Optimizing the photon transport step can be done through a straightforward application of the CADIS method to solve for the SDR at a single location or the FW-CADIS method if the SDR is desired in more than one location. An adjoint transport calculation can be performed where the detector response function is set equal to the photon flux tally fitted with flux-to-dose-rate conversion factors. The resulting adjoint photon flux scored in a region of phase space is equivalent to the importance of that region to the detector response. Therefore, the adjoint flux can be used to determine source and transport biasing parameters.

Optimizing the neutron transport step of R2S, however, is not as straightforward because the importance function needs to represent the importance of the neutrons to the final quantity of interest[7].

### 2.5.1 Multi-Step CADIS

When applied to SDR calculations, the Multi-Step Consistent Adjoint Driven Importance Sampling (MS-CADIS) method aims to increase the efficiency of the neutron transport step using an importance function that

captures the potential of regions to become activated and the importance of the resulting decay photons to the final SDR[7].

The detector response can be expressed as the integral of the importance function,  $I$ , multiplied by the source distribution,  $q$

$$R = \int_V \int_E I(\vec{r}, E) q(\vec{r}, E) dV dE \quad (2.21)$$

MS-CADIS provides a method to calculate an approximation of this importance function where the response is the final response of the multi-step process. In the case of an R2S calculation, the final response is the SDR caused by the decay photons. The SDR is defined as

$$SDR = \langle \sigma_d(\vec{r}, E_p), \phi_p(\vec{r}, E_p) \rangle \quad (2.22)$$

where  $\sigma_d$  is the flux-to-dose-rate conversion factor at the position of the detector and  $\phi_p$  is photon flux. Consider Eq. 2.10 where it was shown that the response  $R$  is equal to the product of the flux and adjoint source. If equation 2.21 is taken to have the same form as Eq. 2.22, and the adjoint photon source is set equal to  $\sigma_d$ , the importance function,  $I$ , is defined as the solution of the adjoint transport equation,  $\phi_p^+$  leading to the following relationship

$$SDR = \langle q_p^+(\vec{r}, E_p), \phi_p(\vec{r}, E_p) \rangle = \langle q_p(\vec{r}, E_p), \phi_p^+(\vec{r}, E_p) \rangle \quad (2.23)$$

The goal of MS-CADIS is to develop an importance function that represents the importance of the neutrons to the final SDR, which is done by setting the neutron adjoint identity equal to the photon response in a relationship equivalent to that shown in 2.23

$$SDR = \langle q_n^+(\vec{r}, E_n), \phi_n(\vec{r}, E_n) \rangle = \langle q_n(\vec{r}, E_n), \phi_n^+(\vec{r}, E_n) \rangle \quad (2.24)$$

Combining these adjoint identities in Eq. 2.23 and 2.24, gives a relationship

$$\langle q_n^+(\vec{r}, E_n), \phi_n(\vec{r}, E_n) \rangle = \langle q_p(\vec{r}, E_p), \phi_p^+(\vec{r}, E_p) \rangle \quad (2.25)$$

In order to solve for the adjoint neutron source,  $q_n^+$ , an equation relating the photon source,  $q_p$ , to the neutron flux,  $\phi_n$ , is needed.

### 2.5.2 Groupwise-Transmutation CADIS

The Groupwise-Transmutation (GT)-CADIS method, an implementation of MS-CADIS solely for SDR analysis, provides a means to do just that [10]. The decay photon source is a result of neutron irradiation and the two quantities can be related by the following definition:

$$q_p(\vec{r}, E_p) = \int_{E_n} T(\vec{r}, E_n, E_p) \phi_n(\vec{r}, E_n) dE_n \quad (2.26)$$

where  $T(\vec{r}, E_n, E_p)$  is a quantity that represents the transmutation process. If an adequate  $T$  can be found, this photon source can be used to solve for the adjoint neutron source in Eq. 2.25.

$$q_n^+(\vec{r}, E_n) = \int_{E_p} T(\vec{r}, E_n, E_p) \phi_p^+(\vec{r}, E_p) dE_p \quad (2.27)$$

The photon source at a single point, Eq. 2.26 can be expressed as this non-linear function of  $\phi_n$

$$q_p(E_p) = \int_{E_n} f(\phi_n) dE_n \quad (2.28)$$

The full transmutation process is complex and would be tedious to capture. As the purpose of calculating  $T$  is only a step in calculating  $q_n^+$  which will be used to generate our biasing parameters, an approximation of the relationship between  $q_p$  and  $\phi_n$  will suffice.

probably  
make  
GT-  
CADIS  
a sub-  
section  
and fill  
out de-  
scrip-  
tion

A series of single energy group irradiations is performed on each material in the geometry. The total number of irradiations performed is the product of the number of materials and the number of neutron energy groups. This results in a photon source that is a function of each neutron energy group. Dividing this photon source by the neutron flux results in the coupling term  $T$ .

GT-CADIS provides an analytical solution to  $T$  when the SNILB criteria are met. It has been shown that for typical FES spectra, materials, and irradiation scenarios, these criteria are met and the following solution of  $T$  is as follows

When met, the photon emission density resulting from the irradiation of a material with a neutron flux is the sum of contributions from each neutron energy group.

Move  
this  
from  
pro-  
posal  
section  
to here

## 2.6 Moving Geometries and Sources

Historically, Monte Carlo analysis of dynamic systems is performed using a series of separate simulations with different input files that contain step-wise changes of the geometry configuration. A new capability that will be available in a future version of MCNP6 allows for the motion of objects, sources, and delayed particles during a single simulation [8], [9]. The Mesh Coupled implementation of the R2S method (MCR2S) [12] developed by the Culham Science Center was updated to allow for geometry components to change location after shutdown.

### 2.6.1 MCNP6 Moving Objects Capability

The moving objects capability in MCNP6 allows for rigid body transformations of objects including rectilinear translations and curvilinear translations and rotations. The objects can move with constant velocity, constant acceleration, or be relocated. Object kinetics are not treated so

the user must use caution and supply transformations that will not cause objects to overlap. This capability is currently applicable to MCNP's native geometry format, constructive solid geometry (CSG) and is not available for mesh-based geometries.

Sources can be assigned to moving objects, therefore can move with the same dynamics as other objects in the problem. This capability also allows for the treatment of secondary particles emitted by objects in motion. This treatment is only approximate because the geometry is fixed during the transport of source or delayed particles. This is a valid approximation due to the assumption that the geometry movement is orders of magnitude slower than particle transport. During the MCNP simulation, source particles are tracked through the geometry from the time of emission to termination. If any of the source particle's interactions result in the creation of a prompt or delayed secondary particle, that information is stored. After the source particle has terminated, any stored secondary particles are retrieved and transported. In the case of delayed particles emitted from moving objects, the location, direction, energy, and time are stored at the time of fission or activation and then at the time of emission, the geometry configuration is updated to provide the correct location and orientation of the delayed particle at the time of emission.

### **2.6.2 MCR2S with Geometry Movement**

The capability of MCR2S that allows for components to change location after shutdown was developed to facilitate SDR calculation during maintenance and intervention activities. MCR2S relies on MCNP for both neutron and photon transport steps and FISPACT for the activation calculations. It allows multiple components to be moved to different locations prior to the photon transport step. These geometry translations occur by creating a copy of the components that will move. Transform cards are applied to the copies. The original components remain in their original locations

and their material is changed to vacuum. Any source particle that starts in one of the components that moves after shutdown is automatically translated to the correct location according to the same transformation. The requirement that both the original component (set as void) and its transformed copy are present during the photon transport step means that there can be no overlap between the parts which could be problematic for small transformations.



## 3 EXPERIMENT

---

### 3.1 Demonstration of GT-CADIS

The GT-CADIS method has proven to be an effective form of VR for calculating the SDR in static FES where the SNILB criteria are met. As it stands, this method will not provide appropriate VR parameters for the cases where there is movement after shutdown. The follow experiment will demonstrate the need for a time-integrated adjoint photon solution in order to provide useful VR parameters for dynamic systems.

#### 3.1.1 Problem Description

The geometry chosen is a simplified representation of a fusion energy device as shown in Fig. 3.1.1. It is composed of a chamber of Stainless Steel 316 (SS-316) with a central cavity measuring 2m x 2m x 2 m. The walls are 2 m thick. The chamber is surrounded by air and there is helium in the central cavity. A CAD model of this geometry was created and tagged with Trellis \*need source\*. A spatially uniform source of 13.8-14.2 MeV neutrons was placed in the central cavity. The total neutron source intensity is  $1.0 * 10^{20}$  n/s. The SDR is measured with a detector 0.5 m outside of the chamber after a single pulse irradiation of  $10^5$  s and decay period of  $10^5$  s. The detector is a sphere, 10 cm radius, located 0.5 m outside of the steel chamber in the x-direction. The material was chosen to be the same as that used in a previous GT-CADIS experiment (52.34 at. % H-1, 47.66 at. % C-12) [10].

First, the R2S workflow was performed in analog (except for implicit capture) and then the GT-CADIS method was used to generate VR parameters to optimize the neutron transport step of R2S.

Figure 3.1: Cutaway view of the geometry. Steel chamber with 2 m thick and central cavity measuring 2 m x 2 m x 2 m. The central cavity is filled with helium and chamber is surrounded by air. A SDR detector is located 0.5 m in the x-direction from the chamber.

Figure 3.2: Neutron flux and relative error resulting from analog MC simulation.

### 3.1.2 Analog R2S

The main steps of the R2S workflow are as follows:

1. MC Neutron Transport
2. Activation Analysis
3. MC Photon Transport

MCNP5 was chosen as the MC code and ALARA the activation code.

First, DAGMCNP5 was run using the CAD geometry generated by Trelis and an input file that contained a Cartesian mesh flux tally over the entire geometry. The flux tally was binned into the 175 group VITAMIN-J energy structure. The resulting neutron flux and relative error for the 13.8-14.2 MeV energy group is shown in Fig. 3.1.2.

PyNE R2S \*need source\* was used to construct the ALARA input files using the neutron flux mesh. ALARA was run using FENDL2.0 nuclear data \*need source\*. PyNE R2S was used again to generate a mesh-based photon source from the ALARA output.

### 3.1.3 GT-CADIS

The steps of the GT-CADIS method used to generate a biased source and weight windows to optimize the SDR at the detector are as follows:

1. Deterministic adjoint photon transport

Figure 3.3: Adjoint photon flux used to generate adjoint neutron source.

Figure 3.4: Adjoint neutron flux used to generate the biased source and weight windows.

2. Calculation of the GT-CADIS adjoint neutron source
3. Deterministic adjoint neutron transport
4. Generation of biased source and weight windows from adjoint neutron flux

PARTISN was chosen as the deterministic code to perform the adjoint transport steps. The adjoint photon source was a 42 energy group VITAMIN-J discretization of the ICRP-74 flux-to-dose conversion factors. The CAD geometry was discretized onto a conformal Cartesian mesh. The resulting adjoint photon flux mesh is shown in Fig. 3.1.3.

This shows that.....

Next, the coupling term  $T$  is calculated for each material, SS316, air, and helium. This is done by performing separate  $1E5$  s irradiation and  $1E5$  s decay ALARA simulations for each of 175 neutron groups in each of the materials.

This  $T$  is combined with the adjoint photon flux to generate the GT-CADIS adjoint neutron source via Eq. ?? \*need to link documents\*. PARTISN is run again using this adjoint neutron source and the resulting adjoint neutron flux for the \*need energy group\* is shown in Fig. 3.1.3.

This adjoint neutron source functions as an importance map of neutrons to the final SDR. It shows that the region of the steel chamber near the detector have a high flux and are therefore important to the SDR, but the regions on the far side have a low flux and are not as important.

Figure 3.5: Biased neutron source generated with GT-CADIS method.

Figure 3.6: Weight window mesh generated with GT-CADIS method.

Figure 3.7: Neutron flux and relative error resulting from MC simulation using GT-CADIS biased source and weight window mesh.

The adjoint neutron flux is used to generate the biased source and weight windows via the CADIS method. These are seen in Fig. 3.1.3 and Fig. 3.1.3.

The biased source and weight window files were used to optimize the neutron transport step of R2S. A DAGMCNP5 simulation was performed using these VR parameters and the resulting neutron flux and relative error are shown in Fig. 3.1.3.

ALARA was run using the neutron flux and the same irradiation and decay scenario used to calculate T. A photon source distribution generated is shown in Fig. 3.1.3

## 3.2 Limitations of GT-CADIS for Moving Systems

Consider Fig. 3.1.3. As mentioned, this functions as an importance map of the neutrons to the final SDR at the detector. If the steel chamber was made of modular components that move after shutdown, during the photon decay process, this importance map is no longer valid. For example, if a component of the chamber located on the far side of the detector moves

Figure 3.8: Photon source generated after ALARA activation calculation using the GT-CADIS optimized neutron transport result.

to a location near the detector, the photons produced in that component become important to the SDR at the detector. This also means that the neutrons in this region are important because it is the neutron irradiation that causes the source of photons.

- reproduce adj flux fig, but w/ highlighted "moving" component"
- need to have good statistics in p src regions moving close to detector

## 4 VARIANCE REDUCTION FOR TIME-INTEGRATED MULTIPHYSICS ANALYSIS

---

The Multi-Step Consistent Adjoint Weighted Importance Sampling (MS-CADIS) method of variance reduction is used to formulate an adjoint neutron source that represents the importance of the neutrons to the final quantity of interest in a coupled, multi-step process. The first implementation of this method was applied to the coupled neutron activation-photon decay process that occurs in FES. Specifically, it was used to optimize the neutron transport step in the ITER SDR benchmark experiment [7]. In its current form, MS-CADIS is only applicable to static systems where the geometry remains unchanged in all steps of the multi-step process.

This chapter will first discuss MS-CADIS outside of the context of SDR analysis. Next, a time-integrated solution to the adjoint of the physical process occurring during geometry movement will be derived. Finally, this time-integrated solution will be applied to the GT-CADIS method to form the TGT-CADIS adjoint neutron source that will optimize the neutron transport step of SDR analysis.

### 4.1 Generalized MS-CADIS Method

In the current literature, MS-CADIS is primarily discussed as it applies to SDR analysis [7]. In actuality, MS-CADIS can be applied to any multi-step process in which the primary radiation transport is coupled to a secondary physical process. The addition of time integration to this methodology can then also be applied to any coupled multiphysics process. For this reason, it is prudent to discuss MS-CADIS in a more generalized manner.

To describe the system of coupled, multiphysics, the operator notation

of the Boltzmann transport equation

$$H\phi = q \quad (4.1)$$

where  $H$  operates on the particle flux  $\phi$  and  $q$  is a source of particles, an equation of the same form that describes a generic secondary physics

$$L\Psi = b \quad (4.2)$$

where  $L$  operates on some function  $\Psi$  and  $b$  is a source term, will be used. The adjoint identity for the neutral particle transport equation,

$$\langle q^+, H\phi \rangle = \langle H^+\phi^+, q \rangle \quad (4.3)$$

where  $\phi$  is the forward and  $\phi^+$  is the adjoint particle flux, and  $q$  is the forward and  $q^+$  is the adjoint source distribution and  $\langle \rangle$  signifies the integration over all dependent variables. This identity is valid for an arbitrary adjoint source function [11], therefore the secondary physics has an adjoint identity of the same form.

$$\langle b^+, L\Psi \rangle = \langle b, L^+\Psi^+ \rangle \quad (4.4)$$

The response of the secondary physics takes the form

$$R = \langle \sigma_b, \Psi \rangle \quad (4.5)$$

According to the CADIS method, if the adjoint source is set equal to the detector response function, the adjoint solution forms the importance function. Substituting  $b^+$  into Eq. 4.5 yields the following

$$R = \langle \Psi, b^+ \rangle \quad (4.6)$$

Combining Eq. ?? with the adjoint identity yields

$$R = \langle \Psi, b^+ \rangle = \langle \Psi^+, b \rangle \quad (4.7)$$

For a coupled, multi-step process, the MS-CADIS method constrains the primary adjoint response such that it is equal to the final response of the system (i.e. the response of the secondary physics) as shown below

$$R = \langle \phi, q^+ \rangle = \langle \phi^+, q \rangle \quad (4.8)$$

Ultimately, the goal is to find a solution for the adjoint transport of the primary radiation transport to use as an importance function for the forward calculation. Therefore, a source for the adjoint radiation transport is needed. Equating the set of adjoint identities in Eq. 4.8 and 4.7, yields the expression in Eq. 4.9.

$$\langle \phi, q^+ \rangle = \langle \Psi^+, b \rangle \quad (4.9)$$

In a practical scenario, the forward source of primary physics (e.g. neutron source resulting from D-T fusion) will be known. The adjoint source of secondary physics is chosen to be the response function for the detector of interest. Given that these sources are known, both solutions,  $\phi$  and  $\Psi^+$  can be found through transport operations. The source of the forward secondary,  $b$ , and adjoint primary physics,  $q^+$ , are both unknown, therefore a second equation is needed. This is a coupled, multi-step system where the source of the secondary physics is a response of the primary radiation transport therefore the two processes can be related by equation 4.10

$$b = \langle \sigma_c, \phi \rangle \quad (4.10)$$

where  $\sigma_c$  is a function that couples the primary and secondary physics.



Consider the process of neutron-induced prompt photon production. In this case, the function,  $\sigma_c$ , is the neutron-gamma production cross section  $\sigma_{n \rightarrow \gamma}$ . The primary focus of SDR analysis is the process of neutron-induced delayed gamma production. GT-CADIS provides a method for calculating  $\sigma_c$  when certain conditions (known as SNILB) hold true. In this case, the coupling term,  $T$ , is an approximation of the transmutation process [10]. As long as there is a solution for  $\sigma_c$ , the function that couples the primary and secondary physics together, there also exists a solution for the adjoint radiation transport source as shown in Eq. 4.11

$$q^+ = \langle \sigma_c, \Psi^+ \rangle \quad (4.11)$$

## 4.2 Time-integrated MS-CADIS

If the configuration of the geometry is changing over time during the secondary physics, it will affect the construction of the adjoint radiation transport source. Instead of a single solution to the adjoint secondary physics, there is a solution at each position and each time represented by the term  $\Phi^+(\vec{r}_v(t), t)$  where  $\vec{r}_v(t)$  refers to the position of volume element,  $v$ , at time,  $t$ . To solve for the adjoint primary source in each volume element  $q_{l,v}^+$ , the time-dependent solutions of the adjoint secondary transport are combined by integrating over time

$$q_{l,v}^+ = \int_t \Psi^+(\vec{r}_v(t), t) \sigma_v(t) dt \quad (4.12)$$

need to introduce volume element

## 4.3 Time-integrated GT-CADIS

GT-CADIS is an implementation of MS-CADIS that is specific to SDR analysis. It provides a method to calculate a coupling term,  $T$ , that relates

explain only sum, not average, is needed

This assumes that the

the neutron flux to the photon source. Applying time integration to the GT-CADIS methodology results in the following solution for the adjoint neutron source

$$q_{n,v}^+(E_n) = \int_t \phi_{\gamma}^+(\vec{r}_v(t), E_{\gamma}, t) T_v(E_n, E_{\gamma}, t) dt \quad (4.13)$$

$$\phi_{\gamma,v,h}^+ = \sum_{t_{mov}} \phi_{\gamma,v,h,t_{mov}} \quad (4.14)$$

There is a  $T$  value calculated for every volume element for every decay time of interest. For many practical problems,  $T$  will not change over the course of  $t_{mov}$  because the time constants of decay and geometry motion are very different. The motion of components occurs over a very short period of time relative to photon decay. The coupling term  $T_{g,h}$  is found with Eq. 6.2

$$T_{g,h} = \frac{q_{\gamma,h}(\phi_{n,g})}{\phi_{n,g}} \quad (4.15)$$

For practical SDR analysis, this integral can be estimated by the sum

$$q_{n,v,g}^+ = \sum_{t_{mov}} \left( \sum_h T_{v,g,h} \phi_{\gamma,v,h,t_{mov}}^+ \right) \quad (4.16)$$

## 5 PROGRESS

---

### 5.1 DAGMC Simulations with Geometry Transformations

#### 5.1.1 Production of Stepwise Geometry Files

A tool has been developed to generate CAD geometry files that capture the movement of components over time. First, a geometry file of the model in its original position is loaded. The geometry components are tagged with transformation numbers that correspond to stepwise transformation vectors that are also given as input to this tool. The position of the components is updated according to these transformations and a new geometry file is produced for each time step. This tool only handles rigid-body transformations and no geometric deformations or scaling. It also does not handle kinetics, so the user must be cautious to not cause any overlap of components during the motion. As an example, consider an activated component of a fusion device that needs to be moved around the facility during a maintenance procedure. The movement of the component would be captured in a stepwise manner and each of the new geometry files generated will be used as the input geometry for the photon transport calculations to determine the SDR at each time step.

#### 5.1.2 DAGMCNP Geometry Transformations

The ability to read transformation (TRn) cards from the MCNP input file and update the position of the geometry has also been added to DAGMC. This capability relies upon the same tagging of components in the CAD geometry file as previously discussed. The transformation will be applied to any geometry component that is tagged with the number on the TR

card. If using this capability to perform stepwise radiation transport calculations over time, the user would create one MCNP input file per time step. Each input file should contain the TR cards necessary to update the position of each component to its new location for that time step. During a DAGMCNP simulation, the geometry is loaded, the MCNP input file is read, the geometry position is updated and then transport is performed.

## 6 PROPOSAL

---

As demonstrated by the experiment in chapter ??, the variance reduction parameters generated by the GT-CADIS method are insufficient for optimizing the neutron transport step of SDR analysis in cases that involve the movement of activated components after shutdown. This chapter will first discuss an implementation plan for adding time-integration to R2S and GT-CADIS. This will cover the propagation of error in SDR analysis and discuss some practical considerations for using these methods. Next, a demonstration of these methods will be proposed. Finally, a summary of goals to accomplish will be given.

### 6.1 TR2S

To produce time-integrated SDR maps, the first two steps of the R2S workflow remain unchanged while a photon transport step needs to be performed at each time-step of geometry movement.

1. MC neutron transport simulation on geometry at time step  $t_{\text{mov}} = 0$
2. ALARA activation analysis
3. MC photon transport simulations on geometry at each time step  $t_{\text{mov}} = 1..N$

The MC neutron transport will be performed on the configuration of the geometry during irradiation. A tetrahedral mesh that conforms to the geometry position at  $t_{\text{mov}} = 0$  is used as a tally to score the neutron flux. This mesh is tagged with the geometry transformations that will occur after shutdown. The tetrahedral mesh neutron flux tally along with an irradiation and decay scenario of interest are given as input to the PyNE R2S script to generate ALARA input files. ALARA is run and produces

photon source files for each decay time of interest. These ALARA photon source files are converted to tetrahedral mesh based sources by another PyNE R2S script. All source mesh files generated will reflect the original position of the geometry. Both the source mesh and DAGMC geometry files are transformed to the correct locations for each  $t_{\text{mov}}$  with the DAGMC transform tool.

## 6.2 Implementation: Time-integrated SDR Analysis

This section introduces a plan to generate fully optimized, time-integrated SDR maps. First, a updated R2S workflow that accounts for the movement of activated geometry components after shutdown is discussed. Then, the implementation of the time-integrated solution to the adjoint photon transport derived in chapter ?? is added to the GT-CADIS process of generating the optimal adjoint neutron source.

### 6.2.1 Generation of the TGT-CADIS Variance Reduction Parameters

A CAD model of the geometry in its original position, that during device operation time, is created. This geometry is tagged with transformation numbers corresponding to the stepwise motion vectors that are applied to move the geometry components along the path from their original to final locations. The DAGMC transformation tool discussed in chapter 5 is used to apply the motion vectors and create HDF5 mesh files of the geometry at each time step. The geometry file at each time step along with the adjoint photon source (the flux-to-dose conversion factors) are given as input into a script that generates a Partisn input file. Deterministic

Need to make the distinction between different times. First, there is the decay time,  $t_{\text{dec}}$  which is the amount of time

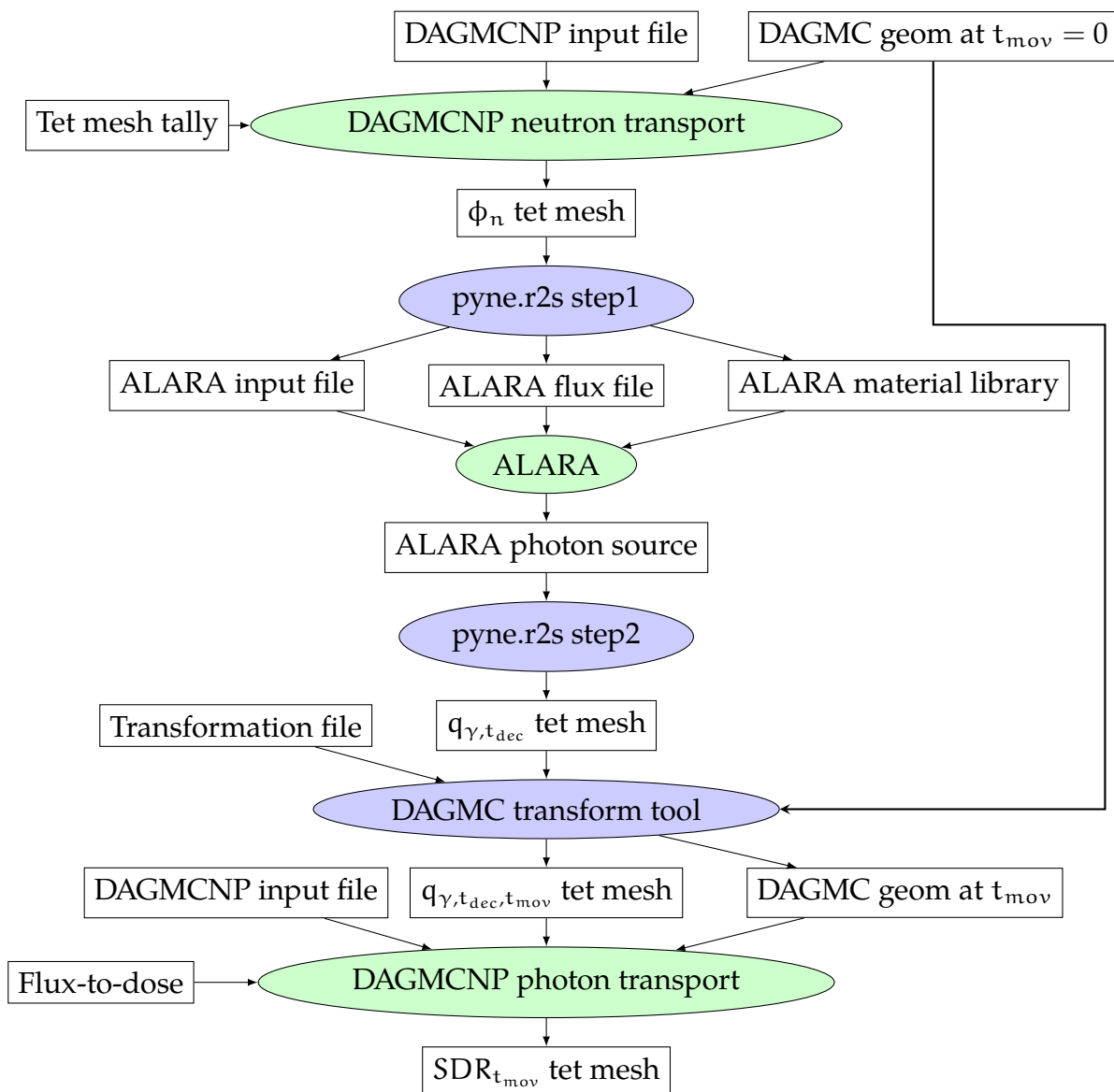


Figure 6.1: Time-integrated R2S (TR2S) workflow for calculating the SDR. Scripts are shown in blue ovals, physics codes in green ovals, and files in white rectangles.

adjoint photon transport is carried out and a Partisn output of the resulting adjoint photon flux is returned. This Partisn output is converted to a an HDF5 structured mesh file through a PyNE conversion method. Because we ultimately need to sum the contribution from each time step in each volume element, the adjoint photon flux voxel mesh is mapped onto the tetrahedral mesh of the geometry at that same time step. Each tet mesh element has an ID associated with it. Those IDs are constant across all geometry files. This allows the contribution of the adjoint flux from each time step to be summed in each tet mesh element.

The time integration is approximated by the following discrete sum over all time steps

$$\phi_{\gamma,v,h}^+ = \sum_{t_{\text{mov}}} \phi_{\gamma,v,h,t_{\text{mov}}} \quad (6.1)$$

The adjoint photon flux tetrahedral mesh is converted back to a voxel mesh to use as input for the PyNE GT-CADIS script. This script ultimately generates a discrete adjoint neutron source for deterministic transport. The coupling term  $T_{g,h}$  is found with Eq. 6.2

$$T_{g,h} = \frac{q_{\gamma,h}(\phi_{n,g})}{\phi_{n,g}} \quad (6.2)$$

To obtain the source of photons in each photon energy group,  $h$ , single pulse irradiations are performed with ALARA. Each material in the problem is irradiated with a single energy group of neutrons,  $g$ , and allowed to decay to the time of interest,  $t_{\text{dec}}$ . The value of  $T_{v,g,h}$  is assigned by finding the material in each voxel,  $v$ . This assumes that  $T$  does not change during the time the geometry is moving,  $t_{\text{mov}}$ .

Combining the calculated  $T$  with the time-integrated adjoint photon



solution, yields the TGT-CADIS adjoint neutron source shown in Eq. 6.3

$$q_{n,v,g}^+ = \sum_{t_{\text{mov}}} \left( \sum_h T_{v,g,h} \phi_{\gamma,v,h,t_{\text{mov}}}^+ \right) \quad (6.3)$$

Once the TGT-CADIS adjoint neutron source has been calculated, deterministic adjoint transport is carried out and an adjoint neutron flux Partisn file is returned. This file is then converted to a voxel mesh. This functions as an importance map for the forward neutron transport. Areas that have a high adjoint neutron flux will have high importance and those with low flux will have low importance. This map will reflect the movement of geometry during the decay period. This adjoint neutron flux mesh is used to generate a biased neutron source and a weight window mesh via the CADIS method.

### 6.2.2 Optimized, Time-integrated R2S Workflow

The source mesh file in its updated position along with the previously generated adjoint photon flux mesh are used to generate a biased photon source and weight window mesh are generated via the CADIS method. At this point, there is a biased photon source mesh, a weight window mesh, and a DAGMC geometry for every time step  $t_{\text{mov}}$ . These are all used along with a DAGMC input file that has a photon flux tally modified by flux-to-dose conversion factors as input for the final DAGMCNP photon transport step. This results in a SDR mesh for each  $t_{\text{mov}}$ .

The TGT-CADIS biased source and weight windows can be used to optimize the neutron transport and the CADIS method can be used to optimize each photon transport step. The fully optimized TR2S implementation is shown in ??.

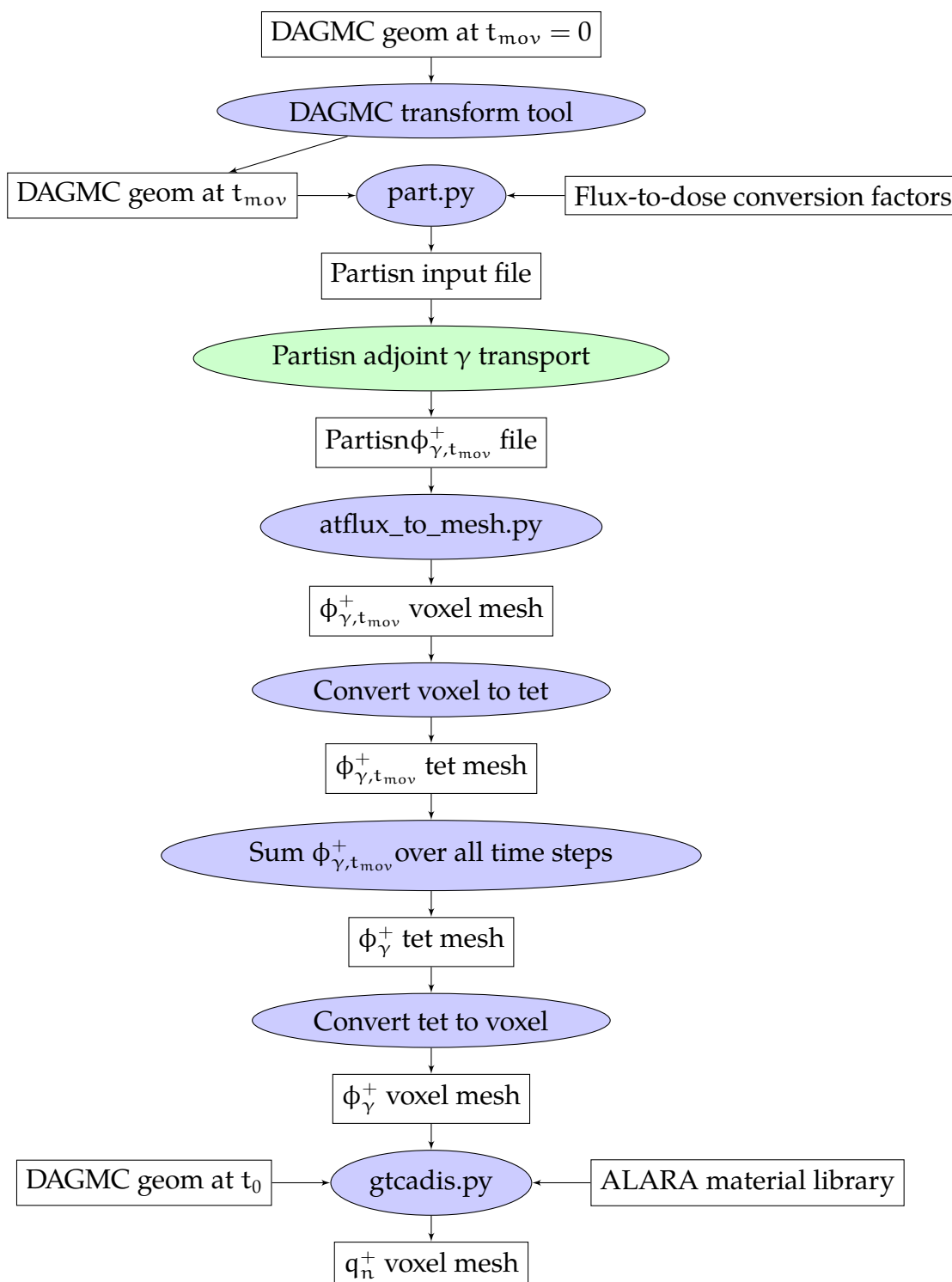


Figure 6.2: Workflow for generating the optimal adjoint neutron source via the time-integrated GT-CADIS method. Scripts are shown in blue ovals, physics codes in green ovals, and files in white rectangles.

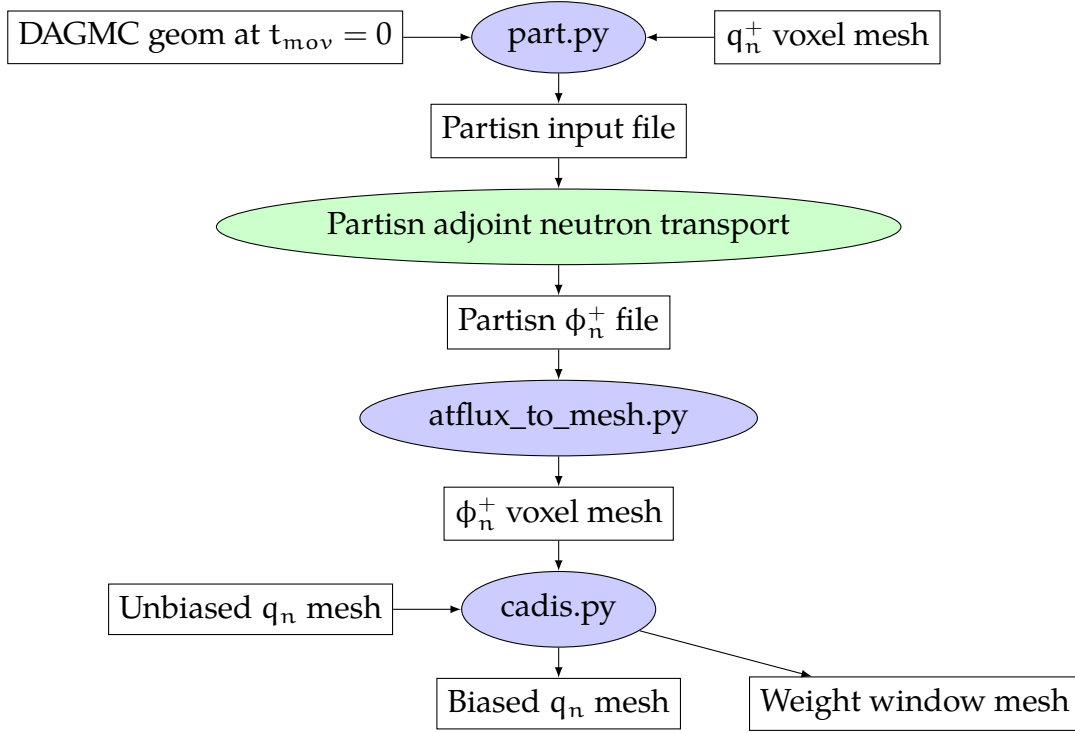


Figure 6.3: Workflow for generating a biased source and weight windows to optimize the neutron transport step. Scripts are shown in blue ovals, physics codes in green ovals, and files in white rectangles.

### 6.2.3 Error Propagation

The total statistical error in the the SDR arises from the MC calculations of the neutron and photon flux.

$$\sigma_{\text{SDR}}^2 = \sigma_n^2 + \sigma_\gamma^2 \quad (6.4)$$

The uncertainty in the SDR due to the uncertainty in the photon transport can be calculated during MC transport. However, the uncertainty in the SDR due to the uncertainty in the neutron MC calculation is more complicated and an area of research currently under investigation by Harb

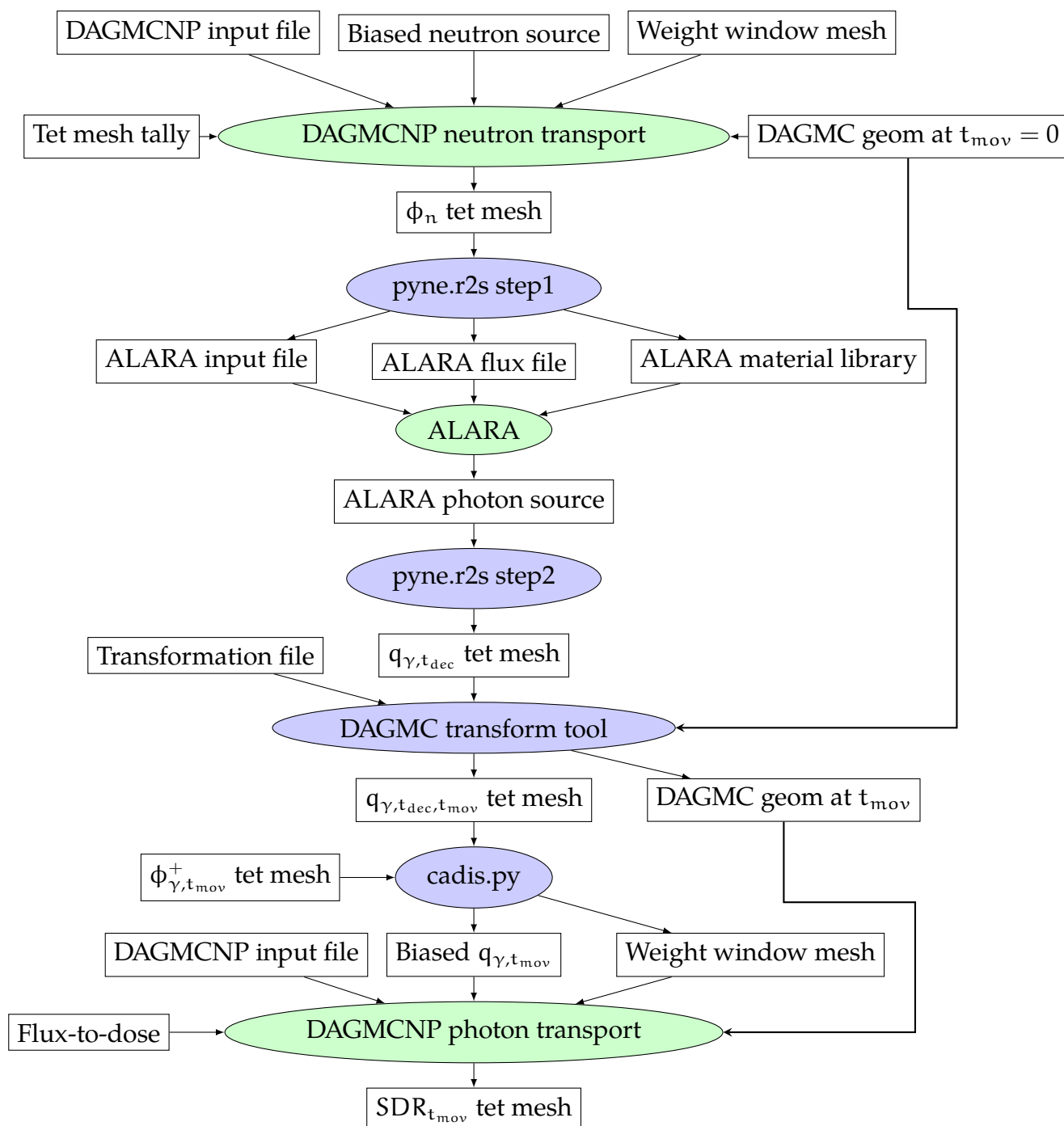


Figure 6.4: Fully-optimized, time-integrated R2S workflow for calculating the SDR. This particular flow chart shows the use of a biased source and weight windows to optimize both neutron and photon transport steps. Scripts are shown in blue ovals, physics codes in green ovals, and files in white rectangles.

et. al. This work aims to produce a methodology for propagating the error from the neutron transport to the photon source and then from the photon source to the SDR.

If a full R2S simulation is carried out, the final SDR has an error associated with the MC neutron photon transport steps. Introducing error from the photon transport step can be avoided by not performing MC photon transport and calculating the SDR using Eq. ?? \*need eqn from background\*.

$$\text{SDR}_v = \phi_{\gamma,v}^+ q_{\gamma,v} \quad (6.5)$$

where  $\text{SDR}_v$  is the response from a discrete volume element,  $v$ . Recall that  $\phi_{\text{gamma},v}$  is the result of the sum of adjoint photon flux over all time steps and required to form the TGT-CADIS adjoint neutron source and  $q_{\gamma,v}$  is the photon source produced by ALARA, so both quantities are already available.

There is some relative error associated with the photon source term that originates from the MC forward neutron calculation. The relative error in the SDR,  $\mathfrak{R}_{\text{SDR}}$  is then expressed as

$$\mathfrak{R}_{\text{SDR}} = \frac{1}{\text{SDR}} \sqrt{\sum_v (\text{SDR}_v \mathfrak{R}_{\text{SDR}_v})^2} \quad (6.6)$$

This error in the SDR can then be used to calculate the neutron transport FOM, shown in Eq. ??, which is important to quantifying the usefulness of TGT-CADIS.

$$\text{FOM} = \frac{\text{SDR}^2}{t_{\text{proc}} \sum_v (\text{SDR}_v \mathfrak{R}_{\text{SDR}_v})^2} \quad (6.7)$$

#### 6.2.4 Assumptions and Practical Considerations

There are three very different time scales: photon transport, geometry movement, and decay. Photon transport happens on a much faster time scale than the geometry movement, therefore it is reasonable to performing

radiation transport on static time-steps of geometry. It is also assumed that the time for the photon emission density to change is much longer than the period of time between the initial and final geometry configurations so the same photon source generated for a particular decay time is used for all photon transport steps  $t_{\text{mov}} = 0..N$ . transport steps during the geometry movement. This also allows the same  $T$  to be used at each time step. Discuss need to explore criteria for situations that this new method will effectively optimize the neutron transport step. It is assumed that the source strength does not change during geometry movement, but a metric will need to be defined to be sure this is true. This depends on the length of time between shutdown and geometry movement. Will need to verify that for a certain window of time, perhaps an eight-hour work shift, the source does not change appreciably. In the case that the source strength is changing appreciably during geometry movement, a series of photon sources that capture these changes over time will need to be used. This will also require the calculation of different  $T$  values for each of these time steps. It is also assumed that the geometry is moving at a constant acceleration and therefore geometry is at each position for an equal amount of time. If this was not true, the sum of adjoint photon fluxes would need to be weighted by time.

#### **6.2.4.1 Data management**

Will be generating a geometry file at each time step, 3-D flux maps for every adjoint photon time step, for the adjoint neutron flux, tet mesh for forward neutron flux, tet mesh of photon source. Need to run adjoint photon transport for many time steps, adjoint neutron, then forward neutron then ALARA.

- efficient obb tree
- htc scripts to run many photon MCNP and compile results

Figure 6.5: Geometry to be used in TGT-CADIS Demonstration.

## 6.3 Demonstration

This section will outline the experiments proposed to demonstrate the utility of TGT-CADIS.

### 6.3.1 Toy Problem

The same geometry used in the GT-CADIS experiment shown in ?? will be used to demonstrate the efficacy of TGT-CADIS. The only difference will be a modular component of the chamber located on the far side of the detector will be moved to a location close to the detector.

First, the TR2S process without any MC VR for the neutron or photon transport steps will be applied to this problem. This will ultimately result in a time-integrated dose map. Next, the photon transport steps will be optimized via the CADIS method. This will require deterministic adjoint photon simulations at each time step to produce VR parameters for the forward MC photon transport runs. Finally, TGT-CADIS will be applied to optimize the neutron transport step. The same adjoint photon flux solutions used in the last step can be used to calculate  $T$  which is then used to calculate the adjoint neutron source for adjoint neutron transport which results in the adjoint neutron flux used to produce the VR parameters.

These incremental additions of optimization will be fundamental in assessing the utility of TGT-CADIS.

### 6.3.2 Full-scale FES Model

As the intended purpose of this work is calculating the SDR during a maintenance or intervention activity in a FES, the final challenge problem

will involve TGT-CADIS optimization of the neutron transport step of TR2S for a full-scale FES.

## **6.4 Summary**



## BIBLIOGRAPHY

---

- [1] A. Haghighat and J. C. Wagner, "Monte carlo variance reduction with deterministic importance functions," *Progress in Nuclear Energy*, vol. 42, no. 1, pp. 25–53, 2003.
- [2] L. Carter and E. Cashwell, *Particle-transport simulation with the Monte Carlo method*. Jan 1975.
- [3] X.-. M. C. Team, *MCNP- A General Monte Carlo N-Particle Transport Code, Version 5*. Apr 2003.
- [4] D. Valenza, H. Iida, R. Plenteda, and R. T. Santoro, "Proposal of shutdown dose estimation method by monte carlo code," *Fusion Engineering and Design*, vol. 55, no. 4, pp. 411 – 418, 2001.
- [5] R. Villari and L. P. Davide Flammini, Fabio Moro, "Development of the advanced d1s for shutdown dose rate calculations in fusion reactors," *Transactions of the American Nuclear Society*, vol. 116, pp. 255–258, 2017.
- [6] Y. Chen and U. Fischer, "Rigorous mcnp based shutdown dose rate calculations: computational scheme, verification calculations and application to iter," *Fusion Engineering and Design*, vol. 63, pp. 107 – 114, 2002.
- [7] A. M. Ibrahim, D. E. Peplow, R. E. Grove, J. L. Peterson, and S. R. Johnson, "The multi-step cadis method for shutdown dose rate calculations and uncertainty propagation," *Nuclear Technology*, vol. 192, pp. 286 – 298, 2015.
- [8] J. W. Durkee, R. C. Johns, and L. S. Waters, "Mcnp6 moving objects part i: Theory," *Progress in Nuclear Energy*, vol. 87, no. Supplement C, pp. 104 – 121, 2016.

- [9] J. W. Durkee, R. C. Johns, and L. S. Waters, "Mcnp6 moving objects. part ii: Simulations," *Progress in Nuclear Energy*, vol. 87, no. Supplement C, pp. 122 – 143, 2016.
- [10] E. D. Biondo and P. P. H. Wilson, "Transmutation approximations for the application of hybrid monte carlo/deterministic neutron transport to shutdown dose rate analysis," *Nuclear Science and Engineering*, vol. 187, no. 1, pp. 27–48, 2017.
- [11] E. Lewis and W. Miller, *Computational Methods of Neutron Transport*. American Nuclear Society, Inc., 1993.
- [12] T. Eade, S. Lilley, Z. Ghani, and E. Delmas, "Movement of active components in the shutdown dose rate analysis of the iter neutral beam injectors," *Fusion Engineering and Design*, vol. 98-99, no. Supplement C, pp. 2130 – 2133, 2015. Proceedings of the 28th Symposium On Fusion Technology (SOFT-28).
- [13] R. ALCOUFFE, R. BAKER, J. DAHL, S. TURNER, and R. WARD, "Partisn: A time-dependent, parallel neutral particle transport code system," may 2005.
- [14] T. Tautges, P. Wilson, J. Kraftcheck, B. F Smith, and D. Henderson, "Acceleration techniques for direct use of cad-based geometries in monte carlo radiation transport," may 2009.
- [15] ICRP, "Conversion coefficients for use in radiological protection against external radiation," *ICRP Publication 74. Ann. ICRP*, vol. 26, pp. 3–4.